Applied Catalysis B: Environmental 123–124 (2012) 69–77

Contents lists available at SciVerse ScienceDirect

Applied Catalysis B: Environmental

journal homepage: www.elsevier.com/locate/apcatb

Optimization synthesis of carbon nanotubes-anatase TiO_2 composite photocatalyst by response surface methodology for photocatalytic degradation of gaseous styrene

Jiangyao Chen[a,c], Guiying Li[a], Yong Huang[a,c], Haimin Zhang[b], Huijun Zhao[b], Taicheng An[a,*]

[a] State Key Laboratory of Organic Geochemistry, Guangdong Key Laboratory of Environmental Resources Utilization and Protection, Guangzhou Institute of Geochemistry, Chinese Academy of Sciences, Guangzhou 510640, China
[b] Centre for Clean Environment and Energy and Griffith School of Environment, Griffith University, Gold Coast Campus, QLD 4222, Australia
[c] Graduate School of Chinese Academy of Sciences, Beijing 100049, China

ARTICLE INFO

Article history:
Received 10 February 2012
Received in revised form 12 April 2012
Accepted 14 April 2012
Available online 21 April 2012

Keywords:
MWCNTs based composite photocatalyst
Optimization synthesis
Center composite design
Photocatalytic degradation
Gaseous styrene

ABSTRACT

In present study, the center composite design in response surface methodology (RSM) was firstly applied to optimize the synthesis of multi-wall carbon nanotubes (MWCNTs)–TiO_2 composite photocatalyst. Twenty-eight composite photocatalysts were prepared by adjusting four operating parameters (amount of MWCNTs, amount of TiF_4, hydrothermal temperature and hydrothermal time) at five levels by the method of multiple variable analysis. The structural, optical and morphological properties of the prepared composite photocatalysts were characterized by X-ray diffraction, UV–visible absorption spectra and scanning electron microscopy, respectively. Based on the experimental design, a semi-empirical expression was firstly established and subsequently applied to predict the photocatalytic degradation activity of the prepared composite photocatalysts to gaseous styrene in a cubic flow-through reactor. The results showed that the experimental photocatalytic degradation efficiencies using the differently prepared MWCNTs–TiO_2 composite photocatalysts matched with the theoretically predicted values very well with a high correlation ($R^2 = 0.9790$). Based on the theoretical and experimental results, the optimum synthesis parameters for the composite photocatalyst within the experimental ranges were 0.01 g MWCNTs, 0.14 g TiF_4, and 120 °C hydrothermally treated for 87.2 h. The photocatalytic degradation efficiency of gaseous styrene using the MWCNTs–TiO_2 composite photocatalyst synthesized under the optimum parameters reached 74.4%. All these demonstrates that the experimental design and theoretical prediction methods used in this work would have great significance in designing and developing high performance photocatalysts for environmental remediation and solar energy conversion.

1. Introduction

During the last decade, photocatalytic oxidation has become an attractive technology for volatile organic compounds (VOCs) abatement [1–8]. Its appeal lies in its potential to mineralize various VOCs into less toxic or harmless compounds under mild conditions [9,10]. As known, photocatalyst plays an important role in the photocatalytic oxidation process. Among the abundant developed photocatalysts, TiO_2 has been found as the most potential photocatalyst for photocatalytic reactions due to its superior photocatalytic oxidation ability, nonphotocorrosive, nontoxic, and inexpensive characteristics [11–15]. However, relative low photocatalytic degradation efficiency is often obtained due to both the high rate of electron–hole recombination in TiO_2 particles and small specific surface area for the limited adsorption of VOCs. Hence, development of high performance TiO_2-based photocatalysts is still an attractive topic for environmental applications.

Recently, the significant interest has been dedicated to enhance the photocatalytic activity of TiO_2 by doping carbon nanotubes (CNTs) towards photocatalytic degradation of VOCs [16–19]. By using these prepared CNTs–TiO_2 composite as photocatalysts, CNTs can not only act as an electron reservoir to suppress the recombination of photo-generated electron–hole pairs, but also act as an excellent adsorbent for VOCs owing to their hollow and layered structures with large specific surface area, which can subsequently enhance the photocatalytic activity of TiO_2. For instance, Yu et al. [16] synthesized the CNTs–TiO_2 composites with different content of CNTs by the modified sol–gel method, and found that the composites possessed high photocatalytic activity for degradation of acetone in air. Xu et al. [17] prepared CNTs–TiO_2 composite photocatalysts using a simple impregnation method by changing the additive amount of titanium source, and the prepared

* Corresponding author. Tel.: +86 20 85291501; fax: +86 20 85290706.
E-mail address: antc99@gig.ac.cn (T. An).

0926-3373/$ – see front matter © 2012 Elsevier B.V. All rights reserved.
http://dx.doi.org/10.1016/j.apcatb.2012.04.020

Table 1
Values and levels of chosen variables for central composite design.

Variable	Symbol	Coded levels				
		−2	Low (−1)	Center (0)	High (+1)	+2
Amount of MWCNTs (g)	*A*	0.01	0.03	0.05	0.07	0.09
Amount of TiF_4 (g)	*B*	0.02	0.11	0.20	0.29	0.38
Hydrothermal temperature (°C)	*C*	120	150	180	210	240
Hydrothermal time (h)	*D*	12	32	52	72	92

photocatalysts exhibited the enhanced photocatalytic activity for benzene degradation. While Yu et al. [18] embedded different amount of CNTs inside the mesoporous TiO_2 aggregates by a facile one-pot hydrothermal method, and the CNTs–TiO_2 composite displayed higher photocatalytic activity for degrading gaseous acetone than that of pristine TiO_2 counterpart. However, although various CNTs–TiO_2 composites were synthesized using different methods, all these reported works applied the approach of single-variable-at-a-time. Such synthetic approach often varies one of the investigated parameter while keeping others as constants, which is usually unable or time consuming to obtain the optimum conditions for the fabrication of high performance composite photocatalysts due to ignoring the interactions and influence among the synthesized parameters. Therefore, development of an efficient experimental design strategy for fabrication of high performance CNTs–TiO_2 composite photocatalysts is highly desired in the field of environmental remediation.

Response surface methodology (RSM) is one of the experimental design techniques that are commonly used for process analysis and modeling [20–24]. The interactions of possible influencing factors on desired responses can be evaluated with RSM just by using minimum number of designed experiments and then an optimal reaction condition can be much easily accomplished. However, no publications to date have applied the RSM to optimize various affecting preparation factors for the synthesis of CNTs–TiO_2 composite photocatalysts.

In present work, RSM was firstly applied to optimize the synthetic parameters for the hydrothermal preparation of CNTs–TiO_2 composite photocatalysts by changing four controlling factors (amount of CNTs, amount of TiF_4, hydrothermal temperature and hydrothermal time) at five levels. The desired response values (degradation efficiency of styrene) predicted using RSM were compared with experimental photocatalytic degradation efficiencies of gaseous styrene. In addition, the relationship between the photocatalytic activity of the prepared CNTs–TiO_2 composite photocatalysts for degradation of styrene and the synthesis parameters was also discussed based on the experimental results.

2. Experimental

2.1. Central composite design for preparation of photocatalysts

The chemometric approach was performed using a central composite design (CCD). Analysis of the experimental data was supported by the Design-Expert software (trail version 8, Stat-Ease, Inc., MN, USA).

The effects of four independent variables (amount of multi-wall carbon nanotubes (MWCNTs), amount of TiF_4, hydrothermal temperature and hydrothermal time) on the synthesis of MWCNTs–TiO_2 composite photocatalysts were investigated in detail using CCD with the form of RSM, and the photocatalytic degradation efficiency of gaseous styrene was selected as the response. The four chosen variables were converted to dimensionless ones (*A*, *B*, *C*, *D*), with the coded values at levels: −2, −1, 0, +1, +2. The determined values of the variables are presented in Table 1. It should be mentioned that the values of the selected variables were determined according to our preliminary experiments. From the table, it can be seen that the five levels for controlling factors are 0.01, 0.03, 0.05, 0.07 and 0.09 g for the factor *A*, amount of MWCNTs; 0.02, 0.11, 0.20, 0.29 and 0.38 g for the factor *B*, amount of TiF_4; 120, 150, 180, 210 and 240 °C for the factor *C*, hydrothermal temperature; and 12, 32, 52, 72 and 92 h for the factor *D*, hydrothermal time. Thus, a total of 28 experimental runs were performed in present study with four replications at the center point. The complete experimental design matrix and the responses are shown in Table 2.

2.2. Synthesis and characterization of photocatalysts

MWCNTs–TiO_2 composite photocatalysts were prepared using a facile one-step hydrothermal method. In a typical synthesis, MWCNTs (Shenzhen Nanotech Port Co., Ltd., China) was firstly purified by a mixture of concentrated sulfuric acid (95–98%) and nitric acid (65–68%) with a volume ratio of 3:1 under the temperature of 90 °C for 90 min. Then, a given amount of purified MWCNTs was dispersed in 40 mL of TiF_4 aqueous solution (Acros Organics, 99%) with different concentrations. After ultrasonic treatment for 30 min, the mixtures were transformed into Teflon-line autoclave with a volume of 100 mL and kept at selected hydrothermal temperature for different durations. After reaction, the products were collected by centrifuge, and then washed with distilled water thoroughly and finally dried at 80 °C for 8 h.

The synthesized composite photocatalysts were comprehensively characterized by X-ray diffractometer (XRD, Rigaku Dmax X-ray diffractometer), UV–visible spectrophotometer (UV–vis, UV-2501PC) and Scanning electron microscopy (SEM, Quanta 400F).

2.3. Photocatalytic degradation experiments

The photocatalytic activities of the prepared MWCNTs–TiO_2 composite photocatalysts were tested by the degradation of gaseous styrene with the initial concentration of 25 ± 1.5 ppmv operating in a continuous flow mode. In a typical reaction process, 0.1 g of the prepared composite photocatalyst was filled in a custom-made cubic quartz glass reactor with the size of 1.0 cm × 1.0 cm × 0.5 cm, top of which was a 365 nm UV-LED spot lamp (Shenzhen Lamplic Science Co., Ltd) fixed vertically with the distance of 6 cm. Dry air was used as a carrier gas and the total flow rate was 20 mL/min controlled by a flow meter. Before the lamp was switched on, the gaseous styrene was allowed to reach gas–solid adsorption equilibrium. The concentrations of gaseous styrene were analyzed by a gas chromatography (GC-900A) equipped with a flame ionization detector. The temperatures of the column, injector and detector were 110, 230 and 230 °C, respectively. Gas samples were collected at regular intervals using a gas-tight locking syringe (Agilent, Australia), and a 200 μL of gas sample was injected into the column for concentration determination in the splitless mode.

Table 2
Experimental design matrix and the value of responses based on experiment run.

Run	Independent variables				Degradation efficiency (%)	
	A	*B*	*C*	*D*	Experimental	Predicted
1	0.03	0.11	210	32	40.9	40.6
2	0.01	0.20	180	52	46.8	49.3
3	0.05	0.20	120	52	60.5	62.3
4	0.07	0.29	210	72	30.1	31.9
5	0.05	0.02	180	52	35.1	37.4
6	0.07	0.11	210	32	32.3	33.2
7	0.05	0.20	180	52	48.3	48.3
8	0.07	0.29	150	32	40.3	40.7
9	0.03	0.29	210	72	34.1	33.6
10	0.07	0.11	210	72	38.3	37.0
11	0.07	0.11	150	32	38.2	38.1
12	0.05	0.20	240	52	39.2	38.1
13	0.03	0.29	150	72	53.9	52.9
14	0.03	0.29	210	32	33.3	33.1
15	0.07	0.11	150	72	46.2	46.3
16	0.07	0.29	150	72	45.4	45.1
17	0.05	0.20	180	12	38.9	38.0
18	0.07	0.29	210	32	30.4	31.9
19	0.03	0.11	150	32	53.4	51.5
20	0.05	0.20	180	52	48.2	48.3
21	0.03	0.11	150	72	62.3	60.2
22	0.05	0.20	180	52	48.6	48.3
23	0.03	0.29	150	32	47.2	48.0
24	0.05	0.20	180	52	48.1	48.3
25	0.05	0.20	180	92	45.1	46.7
26	0.05	0.38	180	52	30.3	28.7
27	0.03	0.11	210	72	45.3	44.8
28	0.09	0.20	180	52	35.9	34.1

3. Results and discussion

3.1. Model establishment and analysis

Based on the experimental results listed in Table 2, a semi-empirical expression in Eq. (1) which is consisted of 15 statistically significant coefficients is obtained and expressed as follows:

$$Y = 48.30 - 3.79A - 2.16B - 6.03C + 2.17D + 1.54AB + 1.51AC - 0.13AD - 0.97BC - 0.94BD - 1.11CD - 1.65A^2 - 3.82B^2 + 0.47C^2 - 1.49D^2 \quad (1)$$

where Y is the response variable of degradation efficiency of styrene. The A, B, C and D represent four experimental factors, respectively.

The adequacy and significance of this model are discussed as follows. Eq. (1) is used to predict the photocatalytic degradation efficiencies of styrene by the prepared MWCNTs–TiO_2 composites with varied parameters within the selected range, and the experimental as well as predicted values are shown in Table 2. It is found that the predicted degradation efficiencies for styrene from the model match with the experimental values very well. This can be further evidenced by plotting the predicted photocatalytic values against the experimental values as shown in Fig. 1, where the line of the best fit with the slope of 0.9797 and $R^2 = 0.9790$ were obtained. This demonstrates that the established model is very suitable to explain the experimental range studied. Moreover, adjusted R^2 (0.9565, see Table 3) is very close to the corresponding R^2 value, which further confirms the adaptability of this model [20].

In addition to correlation coefficient, the residuals (difference between the values of response from experiment and prediction) can be also applied to evaluate the adequacy of the model. The internally studentized residual plot is given in Fig. S1. It can be seen from Fig. S1a that all residuals are well distributed along the straight line, indicating that there is no severe non-normality. Moreover, Fig. S1b shows that the residuals are also distributed between −3 and +3 without any systematic structure and obvious pattern no matter how the predicted value varies. From these results, it can be concluded that the residuals appear to be a random scatter and the model obtained is adequate to descript the relationship between the degradation efficiency and the synthesis parameters for the preparation of MWCNTs–TiO_2 composites.

Table 3 displays the analysis of variance of the quadratic model, which is also required to test the significance and adequacy of the model [25,26]. If the model is adequacy, F-value (the ratio between the mean square of the model and the residual error) should be greater than the tabulated value of F-distribution for a certain number of degrees of freedom in the model at a level of significance [20]. From Table 3, it is found that the F-value for regression of the degradation model is 43.38, which is much greater than the value of $F_{(14, 13)}$ (2.55) at 95% significance, indicating the adequacy of the model.

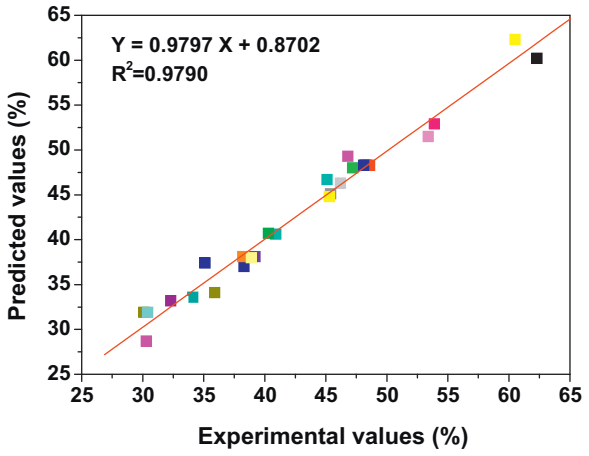

Fig. 1. Correlation between the predicted and experimental degradation efficiencies of styrene by MWCNTs–TiO_2 composite photocatalysts.

Table 3
Analysis of variance for fit of degradation efficiency of styrene.

Source of variations	Sum of squares	Degree of freedom	Mean square	*F*-value
Regression	2006.24	14	143.30	43.38
Residuals	42.95	13	3.30	
Correction total	2049.19			

R^2 = 0.9790, adjusted R^2 = 0.9565.

In order to find out the importance of the selected factors in Eq. (1), the Pareto analysis is also used and the percentage effect of each variable on the response can be calculated according to the following relation [27]:

$$P_i = \left(\frac{a_i^2}{\sum a_i^2}\right) \times 100 (i \neq 0) \quad (2)$$

where P_i represents the percentage effect of each variable and a_i represents statistically significant coefficients in Eq. (1), respectively.

The corresponding results of the Pareto graphic analysis is shown in Fig. 2. As can be seen from the figure, the most important parameter for the preparation of MWCNTs–TiO_2 composite photocatalysts with high degradation efficiency for styrene is hydrothermal temperature (*C*, 41.5%), followed by the amount of MWCNTs (*A*, 16.4%), while hydrothermal time (*D*, 5.4%) and amount of TiF_4 (*B*, 5.3%) play less important roles in this work. Moreover, the degradation efficiency is also affected by the interrelated variables such as two factor interactions (B^2, 16.7%).

3.2. Analysis of contour and response surface plots

The two-dimensional contour and three-dimensional response surface plots are constructed by using the statistical software to illustrate the interaction effects of selected factors on the degradation efficiency and finally find out the optimal parameters for synthesis of MWCNTs–TiO_2 composite photocatalyst with the highest degradation efficiency of styrene. All plots are shown in Fig. 3. Moreover, in order to establish the relationship between the synthesis parameters and the degradation efficiency, the XRD patterns, UV–vis absorption spectra and SEM images of some typically prepared MWCNTs–TiO_2 composite photocatalysts are also displayed in Figs. 4–9.

Fig. 3a illustrates the effect of the amount of MWCNTs and hydrothermal temperature on the degradation efficiency of styrene (amount of TiF_4, 0.20 g; hydrothermal time of 52 h). As can be seen that, when the amount of MWCNTs increases from 0.01 to 0.05 g, the degradation efficiency slightly increases from 46.8 to 48.3% and peaks at 48.3%. However, with further increase of the amount of MWCNTs to 0.09 g, the degradation efficiency decreases significantly to 35.9%. Proper explanation can be obtained from the characteristic results shown in Figs. 4a, 5a and 6. When 0.01 g MWCNTs is added into the composite photocatalyst, the resulted composite photocatalyst is consisted of MWCNTs (unable to be detected by XRD due to the low content) and anatase TiO_2 spheres with the average diameter of about 800 nm. Further observation indicates that the TiO_2 spheres are covered by well-defined exposed crystal facets (see insert of Fig. 6a), which are convenient for the light reflecting/scattering and lead to high light harvesting efficiency [28]. With increasing the content of MWCNTs to 0.05 g, besides the characteristic peaks of anatase TiO_2, a small peak at $2\theta = 26.0^\circ$ for MWCNTs can be observed from the XRD pattern (see Fig. 4a), and the average diameter of TiO_2 spheres is maintained at about 800 nm while the well-defined exposed {0 0 1} crystal facets on the TiO_2 spheres are hardly discerned (see Fig. 6b). Moreover, the UV absorption intensity slightly decreases (see Fig. 5a), which may be due to the disappearance of the well-defined exposed {0 0 1} crystal facets and the increase of amount of MWCNTs preventing TiO_2 from light absorption. On the other hand, the increase of the amount of MWCNTs can also enhance the adsorption and enrichment capacity of the composite photocatalyst to organics [29]. As known, the adsorption of pollutants onto the photocatalyst surface is the first step of photocatalytic reaction, and the higher the adsorption capacity was, the greater the photocatalytic reaction rate constant was [8]. Herein, the increase of the photocatalytic degradation efficiency for styrene is positive correlated with the amount of MWCNTs (within the range of 0.01–0.05 g), which may be attributed to higher increase of the synergetic effect (due to the increase of the adsorption capacity) than the decrease of the UV absorption ability. However, with further increasing the content of MWCNTs to 0.09 g, MWCNTs can be easily detected in the prepared composite photocatalyst by XRD (the diffraction peak at $2\theta = 26.0^\circ$ for MWCNTs). Moreover, few TiO_2 particles can be observed which are covered by the excess MWCNTs (see Fig. 6c), leading to the further decrease of the absorption intensity in the UV region due to the shielding of the UV light for the absorption by TiO_2 with excess MWCNTs, and thus resulting in the decrease of the degradation efficiency.

In the case of hydrothermal temperature, it is found from Fig. 3a that the degradation efficiency continuously decreases from 60.5 to 39.2% with the increase of the hydrothermal temperature from 120 to 240 °C. This result may be attributed to the different structural, optical and morphological properties of the composite photocatalysts as displayed in Figs. 4c, 5c and 7. From Fig. 4c, it can be seen that all composite photocatalysts show the similar XRD patterns no matter how the hydrothermal temperature changes, indicating that low hydrothermal temperature such as 120 °C is enough for the formation of the MWCNTs-anatase TiO_2 composite photocatalysts. However, the average diameter of the TiO_2 particles in the composite photocatalyst sharply increases from about 400 to 800 nm with increasing the hydrothermal temperature from 120 (see Fig. 7a) to 180 °C (see Fig. 7b), and continuously increases to about 1 μm when the hydrothermal temperature further increases to 240 °C (see Fig. 7c). On the contrary, the continuous decrease

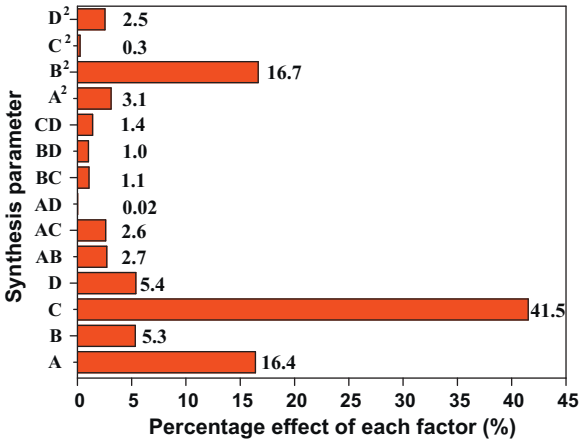

Fig. 2. Pareto graphic analysis for the degradation efficiency of styrene by MWCNTs–TiO_2 composite photocatalysts.

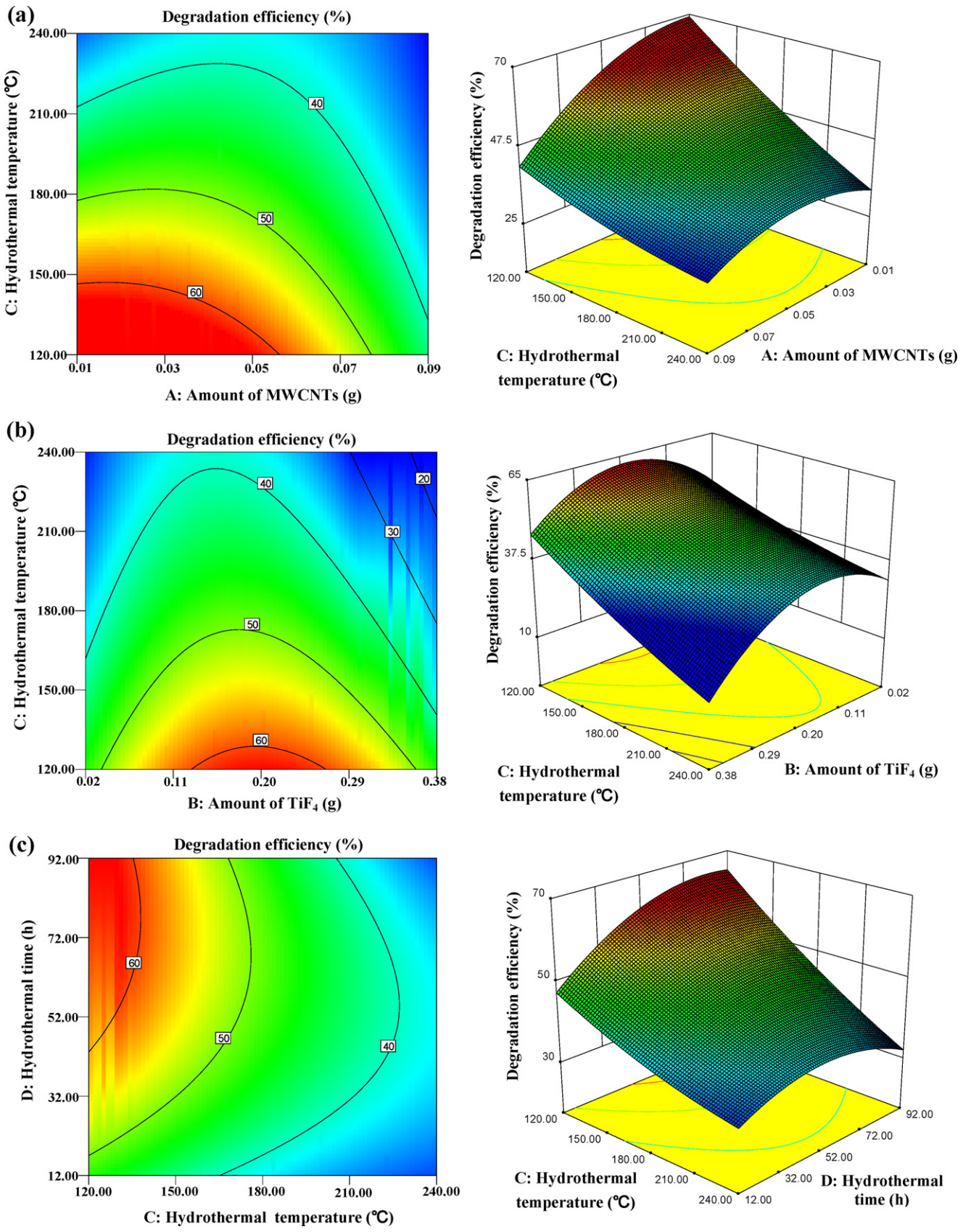

Fig. 3. The contour and response surface plots of degradation efficiency of styrene by MWCNTs–TiO_2 composite photocatalysts as the function of (a) amount of MWCNTs with hydrothermal temperature, (b) amount of TiF_4 with hydrothermal temperature, and (c) hydrothermal temperature with hydrothermal time.

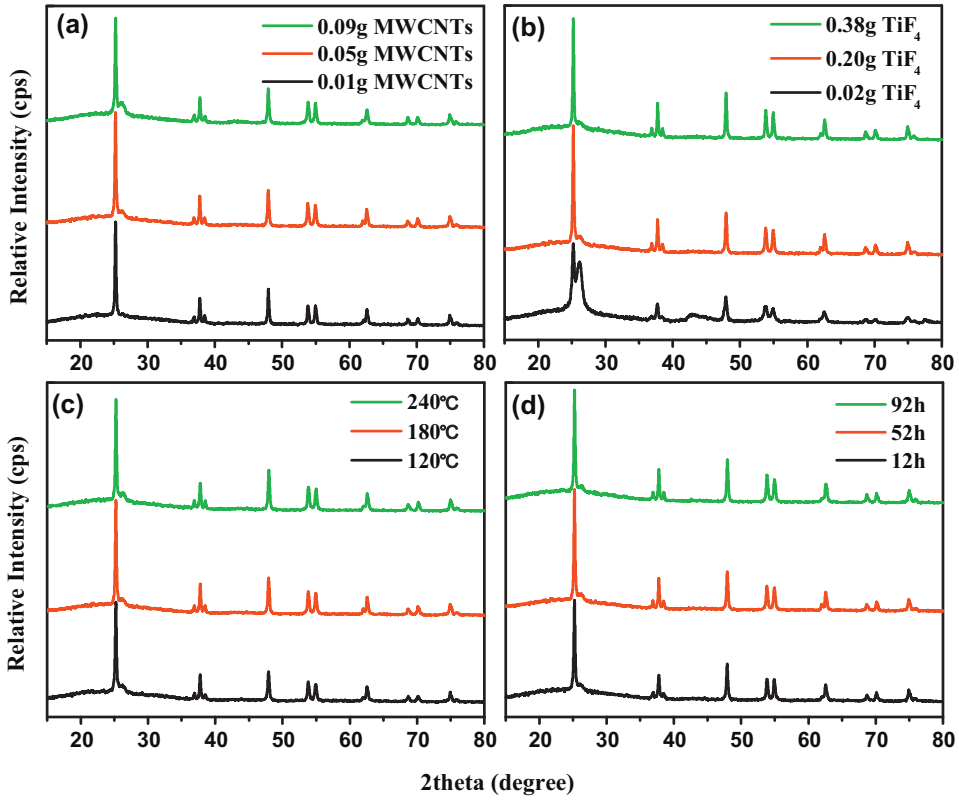

Fig. 4. XRD patterns of composite photocatalysts prepared with different (a) amount of MWCNTs (the amount of TiF_4, 0.20 g; hydrothermal temperature, 180 °C; hydrothermal treatment for 52 h); (b) amount of TiF_4 (the amount of MWCNTs, 0.05 g; hydrothermal temperature, 180 °C; hydrothermal treatment for 52 h); (c) hydrothermal temperature (the amount of MWCNTs, 0.05 g; the amount of TiF_4, 0.20 g; hydrothermal treatment for 52 h); (d) hydrothermal time (the amount of MWCNTs, 0.05 g; the amount of TiF_4, 0.20 g; hydrothermal temperature, 180 °C).

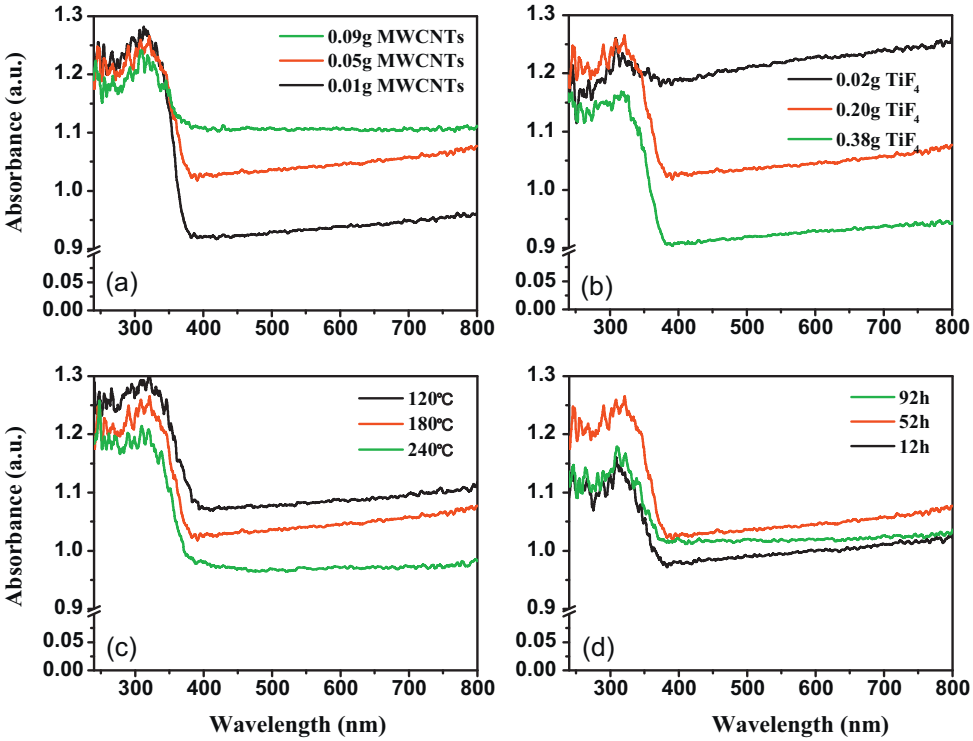

Fig. 5. UV–vis absorption spectra of composite photocatalysts prepared with different (a) amount of MWCNTs (the amount of TiF_4, 0.20 g; hydrothermal temperature, 180 °C; hydrothermal treatment for 52 h); (b) amount of TiF_4 (the amount of MWCNTs, 0.05 g; hydrothermal temperature, 180 °C; hydrothermal treatment for 52 h); (c) hydrothermal temperature (the amount of MWCNTs, 0.05 g; the amount of TiF_4, 0.20 g; hydrothermal treatment for 52 h); (d) hydrothermal time (the amount of MWCNTs, 0.05 g; the amount of TiF_4, 0.20 g; hydrothermal temperature, 180 °C).

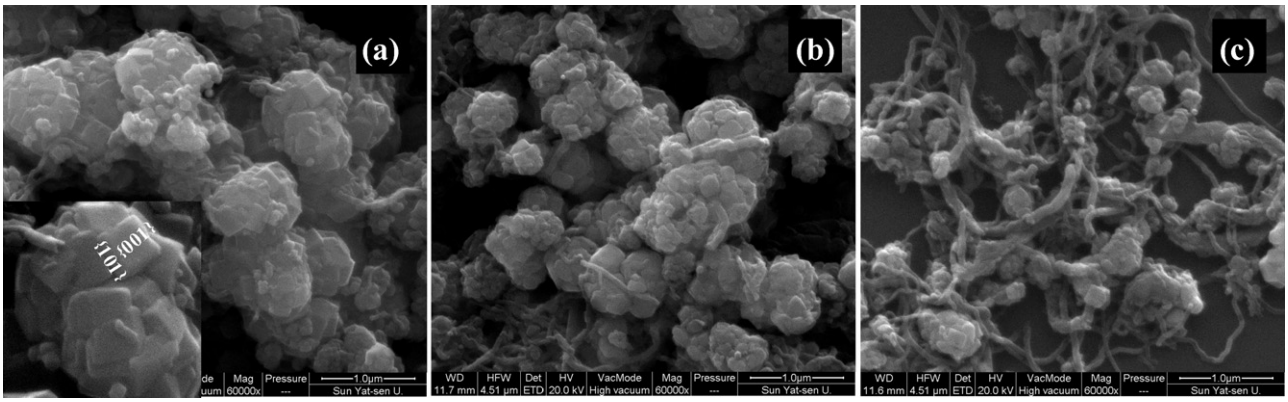

Fig. 6. SEM images of composite photocatalysts prepared with 0.20 g TiF_4, hydrothermal temperature of 180 °C, hydrothermal time of 52 h, and (a): 0.01 g; (b): 0.05 g; (c): 0.09 g MWCNTs.

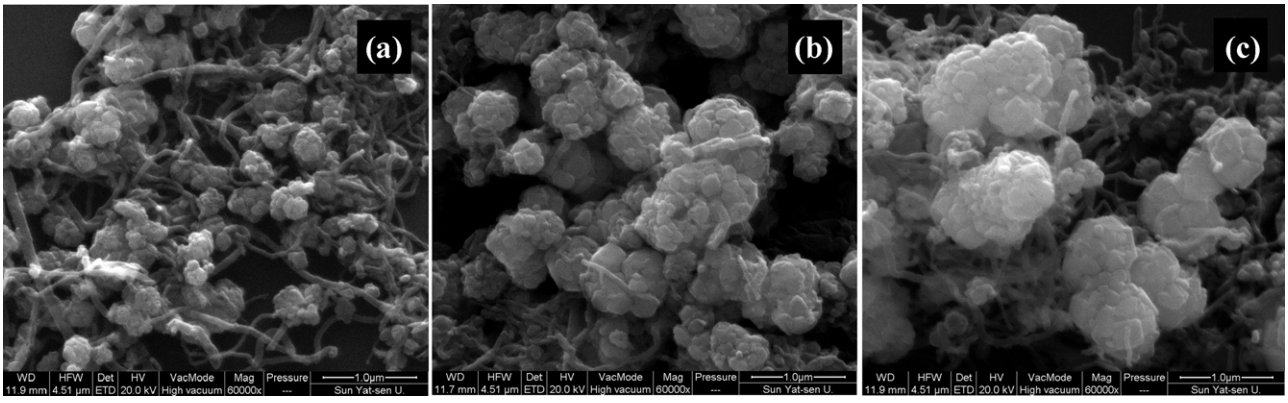

Fig. 7. SEM images of composite photocatalysts prepared with 0.05 g MWCNTs, 0.20 g TiF_4, hydrothermal time of 52 h and hydrothermal temperature of (a): 120 °C; (b): 180 °C; (c): 240 °C.

of UV absorption intensity is observed with the increase of the hydrothermal temperature from 120 to 240 °C (see Fig. 5c). All above-mentioned results indicate that the MWCNTs–TiO_2 composite photocatalyst with smallest TiO_2 spheres and highest UV absorption ability, which possesses the best photocatalytic activity towards degradation of styrene, was synthesized under lowest hydrothermal temperature. This is because that the large specific area of small-sized TiO_2 particles ensures efficient UV light absorption and provides more photoreactive sites for degradation reactions [17]. Furthermore, it was found that lower hydrothermal temperature was in favor of synthesizing composite photocatalyst with larger specific surface area, leading to higher photocatalytic performance [30]. Therefore, the highest degradation efficiency is obtained for the MWCNTs–TiO_2 composite prepared with a suitable amount of MWCNTs addition and minimum hydrothermal temperature (120 °C).

Fig. 3b shows the effect of amount of TiF_4 and hydrothermal temperature on the photocatalytic degradation efficiency of styrene (amount of MWCNTs, 0.05 g; hydrothermal time, 52 h). Similar to the result obtained above, the highest degradation efficiency is achieved when the hydrothermal temperature is maintained at its minimum (120 °C). In the case of amount of TiF_4, there is a notable increase in degradation efficiency from 35.1 to 48.3% with increasing the amount of TiF_4 from 0.02 to 0.20 g. However, further

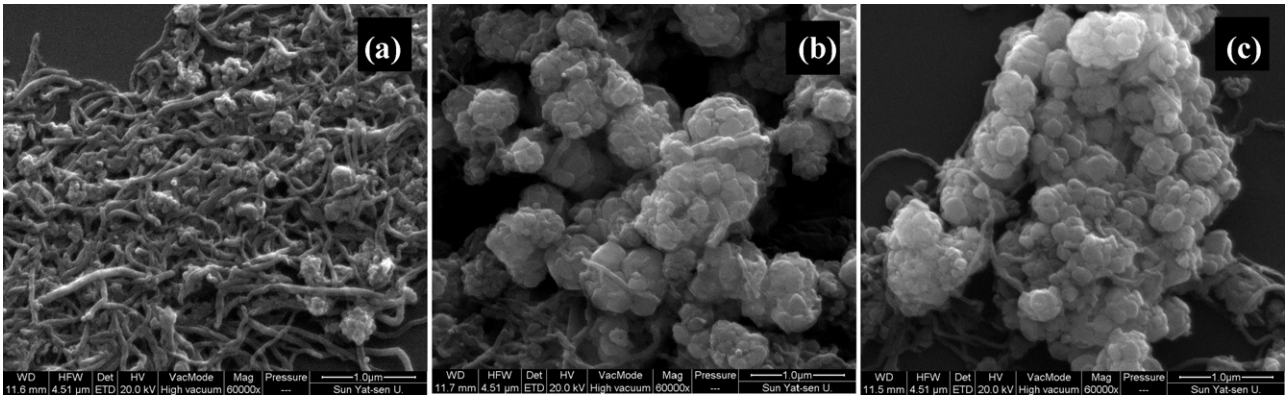

Fig. 8. SEM images of composite photocatalysts prepared with 0.05 g MWCNTs, hydrothermal temperature of 180 °C, hydrothermal time of 52 h, and (a): 0.02 g; (b): 0.20 g; (c): 0.38 g TiF_4.

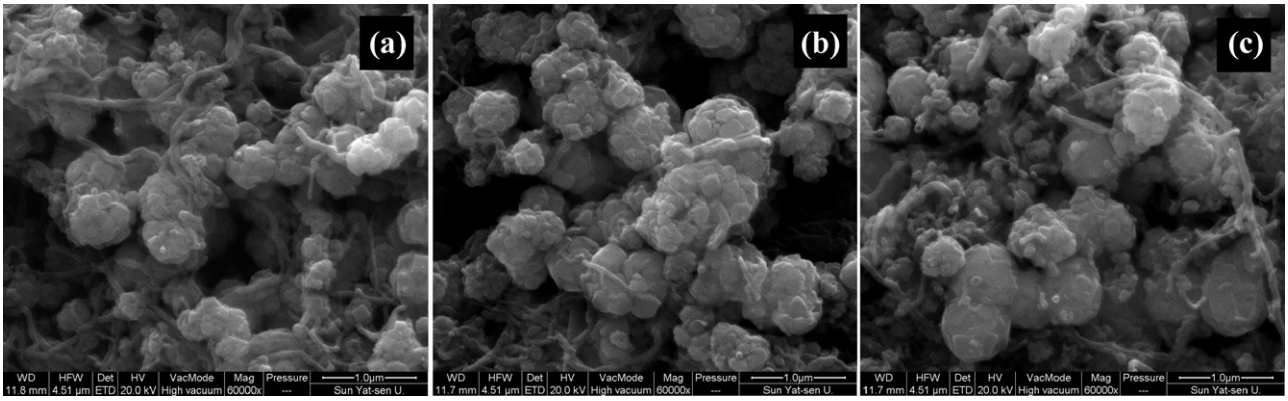

Fig. 9. SEM images of composite photocatalysts prepared with 0.05 g MWCNTs, 0.20 g TiF_4, hydrothermal temperature of 180 °C and hydrothermal time of (a): 12 h; (b): 52 h; (c): 92 h.

increase of the amount of TiF_4 to 0.38 g can lead to the decrease of the degradation efficiency to 30.3%. From the results of XRD patterns (Fig. 4b) and SEM images (Fig. 8) of the MWCNTs–TiO_2 composite photocatalysts, it is clear to see that the intensity of diffraction peak at $2\theta = 26.0^\circ$ for MWCNTs is rapidly weakened and more TiO_2 particles can be observed in the composites with the increase of the amount addition of TiF_4 from 0.02 to 0.20 g (see Fig. 8a and b), leading to the increase of the absorption intensity in the UV region (see Fig. 5b), which is attributed to the electron transition of TiO_2 from the valence band to conduction band [31]. However, with further increasing the amount addition of TiF_4 to 0.38 g, the TiO_2 particles in the composite agglomerate to form large particles with size of about several micrometers (see Fig. 8c) and the UV absorption intensity decreases rapidly (see Fig. 5b) due to the decrease of specific surface area. All these confirm that the composite photocatalyst prepared with lower or higher amount addition of TiF_4 possesses worse photocatalytic activity in this work.

To investigate the effect of hydrothermal temperature and hydrothermal time on the photocatalytic degradation efficiency of gaseous styrene, the degradation experiments are conducted using MWCNTs–TiO_2 composite photocatalysts prepared with different hydrothermal temperature and time varying from 120 to 240 °C and 12 to 92 h, respectively, at constant amount of MWCNTs (0.05 g) and TiF_4 (0.20 g). The results shown in Fig. 3c again indicate that the highest degradation efficiency is obtained when the hydrothermal temperature is kept at its minimum. Moreover, it is found that, with the increase of the hydrothermal time from 12 to 52 and then to 92 h, the degradation efficiency firstly increases steadily from 38.9 to 48.3% and then slightly decrease to 45.1%. The XRD patterns and SEM images shown in Figs. 4d and 9 demonstrate that hydrothermal time has a negligible effect on the structure and morphology of the composite photocatalysts, and the short hydrothermal time of 12 h is enough to form the composite photocatalysts composed of TiO_2 spheres with the average diameter of about 800 nm together with MWCNTs. In addition, it can be seen from Fig. 5d that the absorption intensity in the UV region increases firstly with the increase of hydrothermal time from 12 to 52 h, which may be due to the increased synergistic interaction (for example, the chemical bonding) between TiO_2 particles and MWCNTs [6]. And then the UV absorption intensity decreases when the hydrothermal time is extended to 92 h, though it is even stronger than that of composite photocatalyst prepared with the hydrothermal time of 12 h, implying the synergistic interaction is slightly weakened. This result suggests that UV absorption ability plays a key role during the photocatalytic degradation reaction for the composite photocatalysts prepared with different hydrothermal time, and too short or too long hydrothermal time is not beneficial for synthesizing the composite photocatalyst with higher UV absorption intensity and then higher photocatalytic activity.

To further prove the significant role of the UV absorption ability in the photocatalytic reaction, the XRD patterns, SEM images and UV–vis absorption spectra of MWCNTs–TiO_2 composite photocatalysts with the highest (62.3%, named as composite A) and lowest (30.1%, named as composite B) degradation efficiencies for styrene are compared and shown in Figs. S2–S4 (Supporting Information). Similar XRD patterns are observed for composite A and B (see Fig. S2). However, obvious difference can be discerned from the SEM images (see Fig. S3) and UV–vis absorption spectra (see Fig. S4). From Fig. S3, it can be seen that, although the composites A and B are all consist of MWCNTs and TiO_2 spheres, the average diameters of TiO_2 spheres are about 200 and 800 nm, respectively. Apparently, the TiO_2 particles in composite A is much smaller than that in composite B, which results in a stronger UV absorption for composite A (see Fig. S4). To sum up, in the present study, the stronger UV absorption of the MWCNTs–TiO_2 composite photocatalyst controlled by the synthesis parameters is, the higher of the degradation efficiency is obtained for styrene.

Overall, the main objective of the optimization in this study is to effectively obtain the optimum synthesis parameters for the preparation of MWCNTs–TiO_2 composite photocatalyst with highest photocatalytic degradation efficiency of gaseous styrene based on the experimental results. Herein, by using a numerical optimization method in the Design Expert software, the desired goals for all the variables are chosen in the experimental range that the amount of MWCNTs, the amount of TiF_4, hydrothermal temperature and hydrothermal time are in the range of 0.01–0.09 g, 0.02–0.38 g, 120–240 °C and 12–92 h, respectively, while the degradation efficiency is defined as "maximize" with the upper limit of 100% (the theoretical high). Then, the optimum values of the variables for synthesis of MWCNTs–TiO_2 composite photocatalyst with the highest degradation efficiency (74.4%) for styrene are 0.01 g, 0.14 g, 120 °C and 87.2 h for amount of MWCNTs, amount of TiF_4, hydrothermal temperature and hydrothermal time, respectively.

4. Conclusions

In this study, the RSM was firstly applied in the optimizing the synthesis of MWCNTs–TiO_2 composite photocatalyst with the highest photocatalytic degradation efficiency of gaseous styrene. Among the synthesis parameters in the experimental design, the hydrothermal temperature played the most important role to influence the photocatalytic degradation activity of MWCNTs–TiO_2 for gaseous styrene. Lower hydrothermal temperature was beneficial for synthesizing the MWCNTs–TiO_2 composite with higher degradation efficiency for styrene. Meanwhile, other three

synthesis parameters, such as amount of MWCNTs, hydrothermal time and amount of TiF_4 also showed the influence to the degradation efficiency of the composite photocatalysts. Worse photocatalytic degradation efficiency for styrene was obtained when the composite photocatalysts were prepared under these parameters with lower or higher values. By combining the degradation results and physical properties of the prepared composite photocatalysts, it was found that the absorption ability in the UV region determined the photocatalytic activity of the MWCNTs–TiO_2 composite photocatalyst for gaseous styrene. The stronger UV absorption the MWCNTs–TiO_2 composite photocatalyst is, the higher the degradation efficiency for styrene can be obtained. Finally, the optimum values of synthesis parameters were obtained based on the experimental data which were 0.01 g, 0.14 g, 120 °C and 87.2 h for the amount of MWCNTs, the amount of TiF_4, hydrothermal temperature and hydrothermal time, respectively.

Acknowledgements

This is contribution no. 1489 from GIGCAS. This work was supported by the Science and Technology Project of Guangdong Province, China (2009B091300023, 2011A030700003, 2009B030400001, and 2009A030902003), the Cooperation Projects of Chinese Academy of Science with local government (ZNGZ-2011-005) and NSFC (21077104 and 40572173).

Appendix A. Supplementary data

Supplementary data associated with this article can be found, in the online version, at http://dx.doi.org/10.1016/j.apcatb.2012.04.020.

References

[1] T.C. An, M.L. Zhang, X.M. Wang, G.Y. Sheng, J.M. Fu, Journal of Chemical Technology and Biotechnology 80 (2005) 251–258.
[2] L. Sun, G.Y. Li, S.G. Wan, T.C. An, Chemosphere 78 (2010) 313–318.
[3] N. Quici, M.L. Vera, H. Choi, G.L. Puma, D.D. Dionysiou, M.I. Litter, H. Destaillats, Applied Catalysis B-Environmental 95 (2010) 312–319.
[4] T.C. An, L. Sun, G.Y. Li, S.G. Wan, Journal of Molecular Catalysis A-Chemical 333 (2010) 128–135.
[5] L. Sun, T.C. An, S.G. Wan, G.Y. Li, N.Z. Bao, X.H. Hu, J.M. Fu, G.Y. Sheng, Separation and Purification Technology 68 (2009) 83–89.
[6] Y.H. Zhang, Z.R. Tang, X.Z. Fu, Y.J. Xu, ACS Nano 4 (2010) 7303–7314.
[7] M.L. Zhang, T.C. An, J.M. Fu, G.Y. Sheng, X.M. Wang, X.H. Hu, X.J. Ding, Chemosphere 64 (2006) 423–431.
[8] J.Y. Chen, G.Y. Li, Z.G. He, T.C. An, Journal of Hazardous Materials 190 (2011) 416–423.
[9] T.C. An, L. Sun, G.Y. Li, Y.P. Gao, G.G. Ying, Applied Catalysis B-Environmental 102 (2011) 140–146.
[10] M. Sleiman, P. Conchon, C. Ferronato, J.M. Chovelon, Applied Catalysis B-Environmental 86 (2009) 159–165.
[11] M.R. Hoffmann, S.T. Martin, W.Y. Choi, D.W. Bahnemann, Chemical Reviews 95 (1995) 69–96.
[12] M.A. Fox, M.T. Dulay, Chemical Reviews 93 (1993) 341–357.
[13] X. Chen, S.S. Mao, Chemical Reviews 107 (2007) 2891–2959.
[14] J.Y. Chen, X.L. Liu, G.Y. Li, X. Nie, T.C. An, S.Q. Zhang, H.J. Zhao, Catalysis Today 164 (2011) 364–369.
[15] Q. Zhang, J.B. Joo, Z.D. Lu, M. Dahl, D.Q.L. Oliveira, M.M. Ye, Y.D. Yin, Nano Research 4 (2011) 103–114.
[16] Y. Yu, J.C. Yu, J.G. Yu, Y.C. Kwok, Y.K. Che, J.C. Zhao, L. Ding, W.K. Ge, P.K. Wong, Applied Catalysis A-General 289 (2005) 186–196.
[17] Y.J. Xu, Y.B. Zhuang, X.Z. Fu, Journal of Physical Chemistry C 114 (2010) 2669–2676.
[18] J.G. Yu, T.T. Ma, S.W. Liu, Physical Chemistry Chemical Physics 13 (2011) 3491–3501.
[19] N. Bouazza, M. Ouzzine, M.A. Lillo-Rodenas, D. Eder, A. Linares-Solano, Applied Catalysis B-Environmental 92 (2009) 377–383.
[20] A.R. Khataee, M. Fathinia, S. Aber, M. Zarei, Journal of Hazardous Materials 181 (2010) 886–897.
[21] V.A. Sakkas, P. Calza, M.A. Islam, C. Medana, C. Baiocchi, K. Panagiotou, T. Albanis, Applied Catalysis B-Environmental 90 (2009) 526–534.
[22] S.A.V. Eremia, D. Chevalier-Lucia, G.L. Radu, J.L. Marty, Talanta 77 (2008) 858–862.
[23] T. An, J. An, H. Yang, G. Li, H. Feng, X. Nie, Journal of Hazardous Materials 197 (2011) 229–236.
[24] D. Vildozo, C. Ferronato, M. Sleiman, J.M. Chovelon, Applied Catalysis B-Environmental 94 (2010) 303–310.
[25] M. Zarei, A. Niaei, D. Salari, A. Khataee, Journal of Hazardous Materials 173 (2010) 544–551.
[26] H.L. Liu, Y.R. Chiou, Chemical Engineering Journal 112 (2005) 173–179.
[27] A.K. Abdessalem, N. Oturan, N. Bellakhal, M. Dachraoui, M.A. Oturan, Applied Catalysis B-Environmental 78 (2008) 334–341.
[28] H.M. Zhang, Y.H. Han, X.L. Liu, P.R. Liu, H. Yu, S.Q. Zhang, X.D. Yao, H.J. Zhao, Chemical Communications 46 (2010) 8395–8397.
[29] Y. Yu, J.C. Yu, C.Y. Chan, Y.K. Che, J.C. Zhao, L. Ding, W.K. Ge, P.K. Wong, Applied Catalysis B-Environmental 61 (2005) 1–11.
[30] Q.Q. Zhai, T. Bo, G.X. Hu, Journal of Hazardous Materials 198 (2011) 78–86.
[31] G. Liu, L.Z. Wang, H.G. Yang, H.M. Cheng, G.Q. Lu, Journal of Materials Chemistry 20 (2010) 831–843.